UNIVERSITY of CALIFORNIA
SANTA CRUZ

A SPICE ANALYSIS OF ILC LONG-LADDER NOISE

A thesis submitted in partial satisfaction of the
requirements for the degree of

BACHELOR OF SCIENCE

in

PHYSICS

by

Khilesh Mistry

15 June 2013

The thesis of Khilesh Mistry is approved by:

Professor Bruce Schumm
Advisor

Professor Adriane Steinacker
Theses Coordinator

Professor Michael Dine
Chair, Department of Physics

Abstract

A SPICE Analysis of ILC Long-Ladder Noise

BY

Khilesh Mistry

The long-ladder system is a proposed detection scheme to be implemented in the microstrip tracking region of the SiD ILC detector. It introduces a unique readout array aimed to fulfill the tracking needs of an ILC detector while reducing costs and materials of the experiment. Employing a long shaping time front end amplifier and resistive, narrow stripped silicon sensors, the long-ladder array could potentially reach up to 1 meter in length, significantly longer than current readout arrays. We investigated the difference between a lumped sensor approximation and a distributed sensor as one would expect. We questioned the lumped approximation, showing that network effects have a significant and palliative effect on the noise of the system. These network effects, in combination with a reduction of noise from reading out the sensor in a center-tapped configuration make the long-ladder detector a more attractive option for microstrip tracking in the ILC .

Contents

1 Motivation

Originating with Thales, a Greek philosopher, rejecting the notion of mythological and religious explanations of everyday phenomena, physics began as the empirical search for fundamental truths. In the thriving intellectual atmosphere of the Greek classical period, Aristotle carried this thought forward with his theory that everything is made of earth, fire, water, wind, or æther. Aristotle tried to explain what matter was composed of and had the eventual goal of describing the principles of motion. His work paved the way toward the birth of physics as a pure science and our modern way of thinking [1]. He was essentially asking these three questions:

What is the world made of and why?

How did this universe come to be?

How does one fully describe this world?

These questions have driven scientists around the world to discover new, unexpected realities of our world. Initially, revolutionaries like Da Vinci, Galileo, and Newton used their surrounding and simple mechanisms they created to delve deeper into these physical laws. After centuries of promising work, physicists, such as Lord Kelvin, thought there would there be almost nothing left to solve....until the advent of relativity and quantum mechanics at the turn of the 20^{th} century. With this newfound insight, conventional methods for studying matter were becoming less useful as quantum effects were apparent only at unprecedented energies and scales.

That all changed in 1930, with the birth of the first modern particle accelerator. The 500 kilovolt machine, fabricated by John Cockcroft and Ernest Walton, could accelerate protons through a 8 foot long tube to a kinetic energy of 0.7 MeV. With this new design, Walton and Cockcroft were the first to probe the inner structure of a Lithium nucleus, a large step forward in understanding the depths of the atomic structure.

After exponential technological improvement, today's most powerful particle accelerator has more than a million times the energy of the Walton-Cockcroft device. The Large Hadron Collider (LHC), located at CERN (Organisation Européenne pour la recherche nucléaire) in Geneva, Switzerland, was designed as a "discovery" machine. Its purpose is to find the Higgs boson, chart the unexplored landscape of tera-scale physics, and help us refine the Standard Model. In the summer of 2012, the two main experimental collaborations at the LHC, ATLAS and CMS, announced the discovery of a

Higgs-like boson resonance at 126 GeV [2]. This long sought after boson is the primary missing link in our astonishingly accurate model called the Standard Model, which describes the constituents of matter and the interactions mediating them. However, questions about the unification of the electro-weak and strong forces as well as the ad-hoc nature of the model need to be addressed in order to solidify our understandings of the world and firmly cement the Standard Model (SM) as *the* most fundamental description of our universe. Today we are asking the same questions ancient physicists did, just in a different, more refined light:

What is matter and energy?

How do fundamental particles get mass?

What is dark matter?

Do the forces unify?

At first glance these questions may look different from the previous ones. Answering them would provide us with insight about the very early universe, unknown properties and interactions of matter, and hint at physics beyond the Standard Model.

The LHC will prove to be a vital tool in answering these questions as it is designed to collide protons at unprecedented energies of up to 14 TeV. However, there is a very important limitation. Circular "Synchrotron" accelerators accelerate protons, rather than electrons, because particles lose their energy due to synchrotron radiation proportional to the inverse fourth power of mass. At high energies, the energy loss of an accelerating electron is so large that it becomes inefficient to maintain its energy, necessitating protons to be the main elements of synchrotron accelerators. However, protons are composed of other fundamental particles, three valence quarks and a sea of partons (gluons and quarks). This makes collisions at the LHC "messy" as the interactions contain masses of unwanted "colored" byproducts due to the strong nature of the partons which make up the protons (Fig. 1). Therefore the LHC, like other synchrotron hadron colliders, works as a powerful discovery machine, and linear colliders are necessary complements, functioning as precision measurement experiments designed to characterize and study in finer detail the discovered physics.

One planned complement to the LHC is the International Linear Collider (ILC). If built, this proposed experiment will be the largest and most powerful linear collider, covering over 30km. The ILC will collide electrons and their anti-matter counterparts, positrons, with center of mass energies upwards of 500 GeV. Because of the pointlike

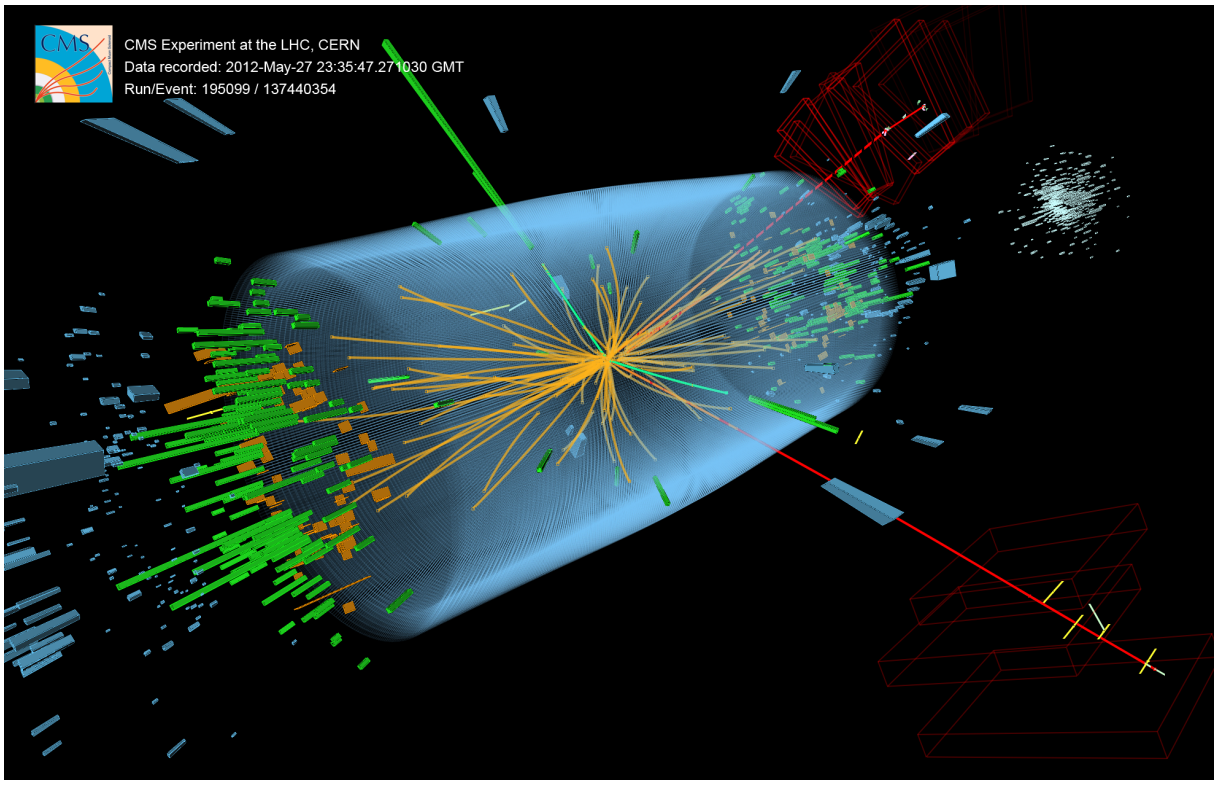

Figure 1: A potential Higgs event in the CMS detector. Notice the slew of excess particles created (all the green and yellow bars near the caps). This the the excess "messy" part of an LHC interaction.

nature of the colliding particles, the collisions would be "cleaner" and easier to study with precision. In particular, the kinematic properties of the intial state are exactly known, providing a powerful constraint for the reconstruction of the final state. Its most important contribution, given the light of a new boson seen at the LHC, will be to study this new particle, but in general the ILC can be used to study any new phenomena discovered at the LHC. Unlike the LHC, the ILC will be able to make exceedingly precise measurements of this new boson's spin and parity, as well as measuring the boson's precise couplings to quarks and other vector bosons. This will be able to elucidate the nature of this particle, revealing whether it is the SM Higgs or something subtly different, thereby pointing the way to a new chapter in the development of the fundamental theory of nature.

At the current time, the ILC's location and final detector designs are still up in the air, but with Japan looking to be a possible host for the project, the ILC collaboration may be heading toward beginning construction of the accelerator within a decade. While final detector designs may still be undecided, the level of precision needed by the experiments is not. The ILC demands ambitious requirements of the performance

and measurement capabilities of the instrumentation. Specifically, the position and path measurements of individual particles resulting from the collision need to be fine enough in order for the momentum to be extracted to a degree of precision commensurate with the intrinsic precision of the ILC machine.

My research focuses on the noise analysis of a new solid-state detector concept, the long-ladder detector, used to track outgoing particles. If the noise can be understood and controlled, the long-ladder can be used to instrument larger volumes with precise solid-state particle tracking. The main focus of my research is to clarify and interpret the discrepancy between analytical and measured noise of the long-ladder system. I investigated the effects of a distributed detector-readout network compared with just a simple RC circuit representation of the detector, as assumed in the analytical calculation used for initial designs of the detection scheme.

In the following sections I discuss the simulation tools and basic concepts that the project is based upon, leading into my development and completion of a computer simulation used to analyze the problem. Subsequent sections then present the refinement to the model and noise measurement results of the long-ladder study.

2 Background

2.1 Silicon Strip Detectors

Silicon sensors are currently the standard for detecting ionizing particles traversing through detectors. They can be used for particle detection as well as radiation detection and are generally very fast due to their inherent nature as a solid state device. Combined with modern lithography to make finely separated strips/pixels, the silicon sensor is the ideal candidate for precise position detection schemes in high energy accelerators.

A typical silicon sensor can be described with basic semiconductor concepts and in its simplest form is a diode. A typical diode is a n-type material, joined together with p-type material at a P/N junction. The free charge carriers near the junction of the materials are swept away by inherent junction properties, creating an electric field at the junction void of free electrons and holes. This region, void of all free charges, is called the depletion region.

As is common with most silicon detectors, the long-ladder sensors consists of doped n-type silicon bulk, with doped p-type implants implanted on the top of the bulk. Aluminum strips are placed on top of the p-type implants, with silicon oxide used to insulate and create a capacitative coupling between the strip and metal. The backside of the n-type bulk was metalized to provide a plane for biasing the diode.

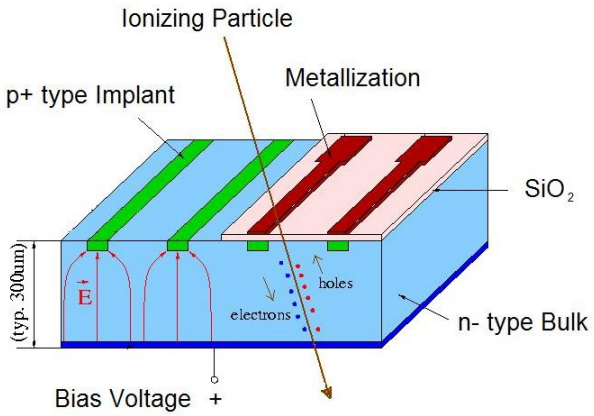

Figure 2: An illustration of a particle traversing a silicon sensor

With this basic setup, by applying a positive potential to the metalized back plane of the sensor, while holding the implanted strips at ground, a reverse biased detector is created. The depletion region in the device will expand with increasing potential, and near 100V the n-type bulk will be fully depleted — void of any roaming charge carriers. As a result of the potential difference being applied between the strips and the back plane, an electric field is induced in the device.

Now with the detector fully depleted, any charged particle that traverses through the 300μm-thick device will create nearly 25,000 electron/hole pairs of which the holes will be swept upward and deposited on the strips while the electrons will be

swept downward, being deposited on the back plane. An illustration of this process can be seen in Figure 2. The charge deposited on the implants can be read out as a signal due to the capacitative coupling to the aluminum strips. With careful detection schemes and the right readout electronics, the position of the traversing particle can be pinpointed to within a few microns.

2.2 SiD Design Concept

The ILC detectors will be immersed in a 5 Tesla magnetic field in order to curve the charged particles being created in the electron-positron collisions. Silicon detectors can pinpoint the position of the traversing particles and with many layers of silicon, the entire trajectory of the particle can be reconstructed. With the particle's trajectory known, the momentum of the particle can be extracted by reconstructing its radius of curvature. Measuring trajectories and radii of curvature to high accuracy will be essential as the particles are only slightly curved due to their high energies. Ideally, precision position measurements to reconstruct tracks need to be exact up to a few microns. Therefore silicon tracking in the ILC needs to be highly robust, and the SiD (Silicon

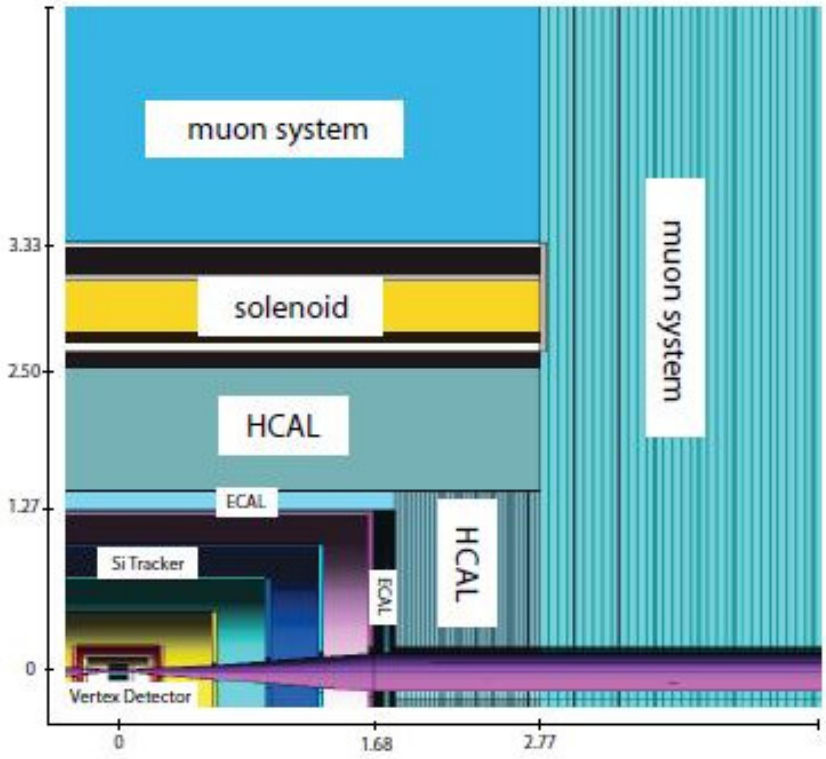

Figure 3: A cross-sectional view of the SiD design concept [3]

Detector) concept is one possible way to address the many problems of detecting high energy particles. The experiment itself consists of 6 onion-like layers moving outward (Fig. 3). In this figure, a cylindrical quadrant is shown moving outward from the center to increasing radius (y axis of figure), with the Z axis of the detector running from the center of the cylinder, to one of its caps (horizontal axis). The first layer is pixel tracking, arranged in 5 sub-layers, right next to the vertex of interaction. After that comes the main silicon microstrip tracking layer, once again composed of 5 sub-layers. This region is where long-ladders can be employed to cover over half the length of these trackers. Seen in Figure 4, the long-ladder detectors are proposed to be used in the silicon barrel region (blue lines). These first two layers (pixel and microstrip tracking) are to capture and record the position of outgoing charged particles, allowing for the reconstruction of their paths. This layer ends 1.27 meters out from the center of the

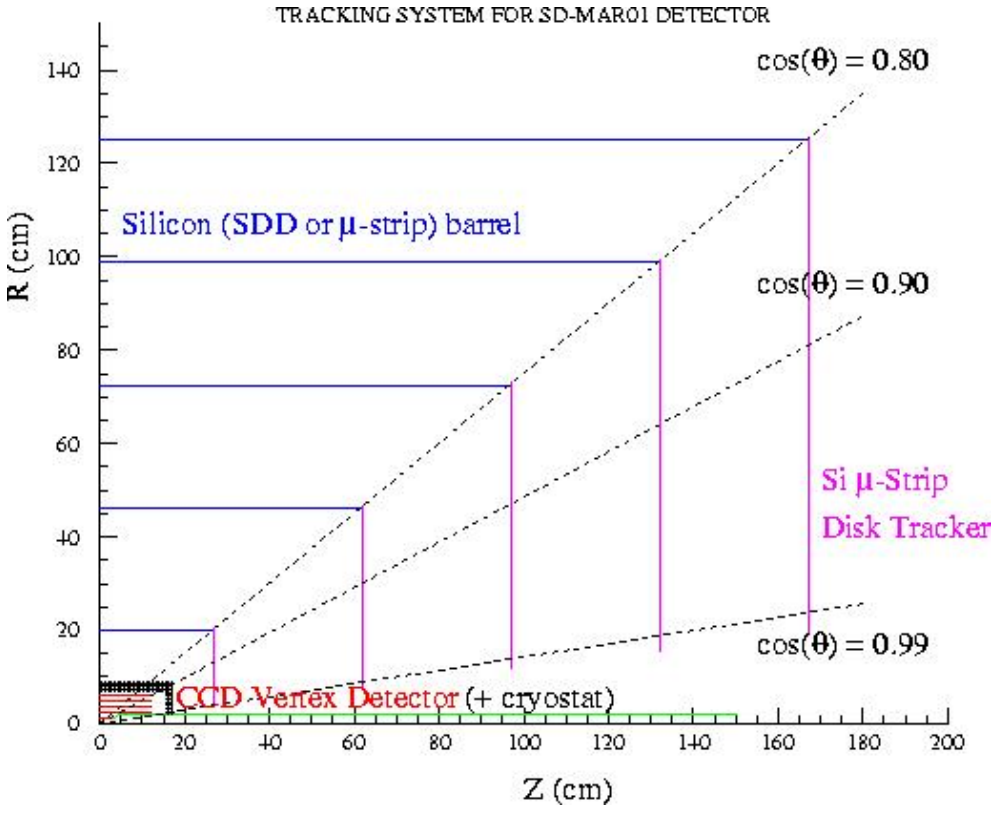

Figure 4: A cross-sectional view of the Silicon Tracker

detector, immediately backed by the Electromagnetic Calorimeter (ECAL). Designed to measure the energy deposition of electromagnetically interacting particles, the ECAL uses a sampling silicon-tungsten calorimeter. The next layer is the Hadronic Calorimeter or HCAL. Its purpose is very similar to the ECAL, but instead of measuring particles

like photons or electrons, it measures the energy of individual hadrons, such as the pion, produced in interactions. These two calorimeter layers are primarily constructed to capture and record the energy of the particles transiting through the detector. The last two layers consist of the large 5 Tesla magnet and muon chambers, arranged to identify these weakly interacting particles as they pass through [3].

This detector would be considerably smaller than the other proposed design concepts, such as the Global Large Detector (GLD) and the Larger Detector Concept (LDC). These detectors focus on Large HCALs and ECALs and the GLD with gaseous barrel tracking. While alternatives provide many more measurements of tracking, the SiD, with its silicon tracking and finer precision, should be able to overcome its lack of measurements compared with competitors. One way to accomplish this would be with the long-ladder detection scheme [3].

2.3 The Long-Ladder Detector

Long-ladder detectors are a proposed solution for reducing the amount of electronics and cabling while maintaining the accuracy of measurements in the microstrip barrel tracking region of the SiD. Long-ladder detectors, as the name suggests, differ from regular silicon sensor applications as the total length of the sensor chain read out by a single electronics channel is much longer. While common silicon strip detectors are less than 10cm long, long-ladder detectors are composed by connecting sensors end to end, in series, or “daisy chaining” them. These detectors can be up to one meter long, and will run off of one set of readout electronics, reducing the amount of electronics and cabling by a factor of more than 10. As promising as this sounds, the application of this type of detector to precision tracking is a recent development and studies of the system’s noise and performance are needed, especially in comparison with naïve noise estimations that theory of this detector concept design was based upon.

Ideally, the long-ladder detector would have been tested by actually daisy-chaining 10+ detectors, and studying this setup. While the first iteration of this study had this setup, the strip pitch (separation) was too wide for precision tracking and so the noise was not dominated by the relevant parameters. A picture of the previous setup can be seen in Figure 5 to visualize the actual design concept. With a new smaller width silicon sensor in hand, it was decided to use one sensor as the “ladder” and study the noise of one long strip.

The individual silicon sensor was a 128-strip sensor with a length of 4.75 cm. On

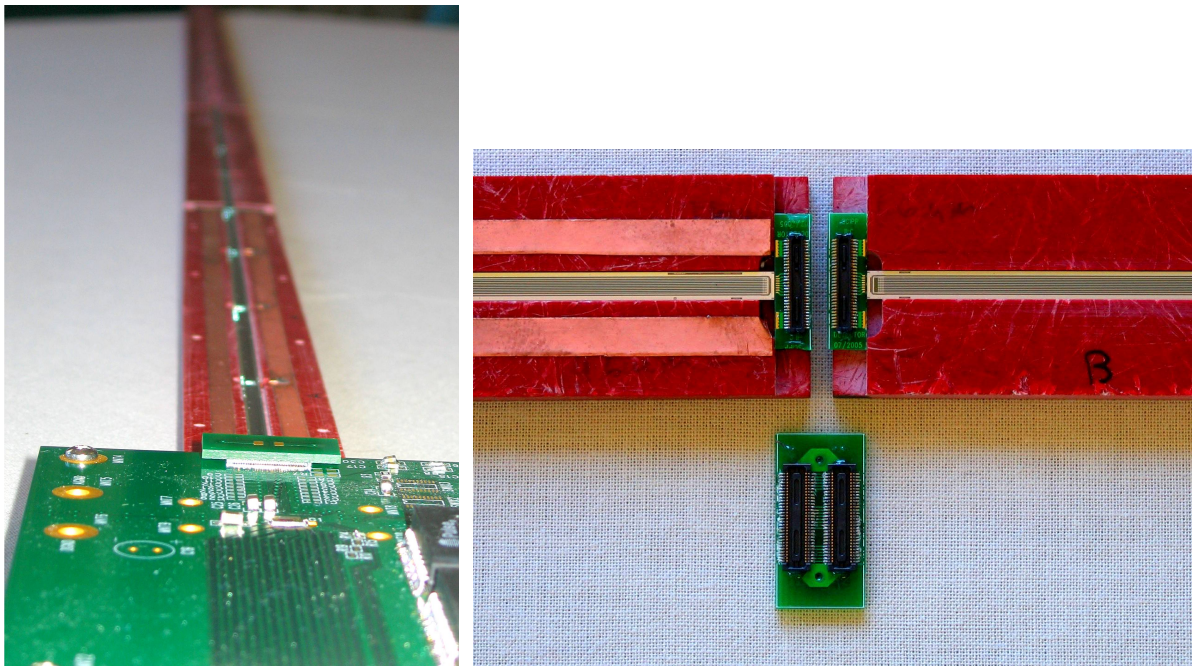

Figure 5: Left — The LSFTE, the circuit board, with the end tapped setup. Note the length of the setup. **Right** — The "daisy-chaining" of the previous long-ladder. Two sensors were connected with pitch adapters

the sensor, 10 strips were grounded between each active one to reduce cross-talk between channels, approximating the effect of being single strips on individual sensors. The strips are then wire-bonded together end to end, and thus the ladder metaphor is realized, as each strip is another rung on this "ladder". The strips themselves are $7\mu m$ wide with a pitch of $50\mu m$. The narrow width in tandem with the $50\mu m$ pitch lead to a substantial single strip resistance of 287 Ω, and a dominant noise source for long-ladder precision sensors. With this setup, ideally, individual position measurements should be able to be made with precision better than $10\mu m$. Each rung of the ladder (each strip in this case) has a capacitance of 5.2 pF, thus with the setup of 13 strips daisy-chained together, the setup had total resistance and capacitance of 3.73 $k\Omega$ and 67.6 pF respectively. The whole array is read out by SCIPP's prototype Long Shaping Time Front End (LSTFE-1) chip.

The LSTFE readout chip is an application specific integrated circuit (ASIC) amplifier currently in a R&D phase of ILC studies. It was designed to have limited dependence of noise as a function of input capacitance for pure capacitive loads, achieved in part with long shaping time readout electronics ($1\mu s$). Shaping time is the time it takes for the beginning of the signal to reach its peak.

The LSTFE has 3 main parts in its chain — the preamp, the differentiator, and the integrators. The preamp is a transimpedance device, converting the charge pulse into a stepfunction voltage signal before shaping. The differentiator and integrators act as high pass and low pass filters respectively and shape the step into a Gaussian excitation with desired properties (e.g shaping time) predetermined by the circuit element values. The time evolution of the signal shaping can be seen in Figure 6.

The LSTFE can be positioned to read the signals from the detector in two ways: center-tapped and end-tapped. End-tapping is placing the LSTFE at the end of the series chain of sensors, while center-tapping is reading out the signals from the middle of the long-ladder. The previous picture shows the setup in the end-tapped configuration (Fig. 5). Both configurations will be explored in this thesis.

A main advantage of the long-ladder concept is its lack of electronics. With the ILC's cycling beam, the electronics of the detector are also planned to be power cycled at 5 Hertz, as to reduce the electrical heat. This, in tandem with the constant 5 Tesla magnetic field, produces a periodic Lorentz force due to the changing current in the electronics. This 5-Hz hammering of the electronics can be detrimental to stability of the mechanical design, and increase uncertainties in measurements. The long-ladder detector can mitigate this problem by requiring less electronics, thereby diminishing this Lorentz force hammering. Less electronics can also mean less material and cabling, further reducing the chance of photon conversion of outgoing particles or scattering of charged particles. This in turn will allow for ultra precise charged particle tracking and momentum reconstruction as well as higher accuracy calorimetry measurements.

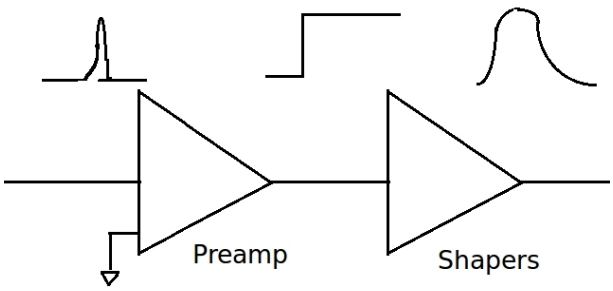

Figure 6: A diagram of a pulse's time evolution as it passes through different parts of the readout. Useful information can be extracted from the final signal

The length of this system, though it has many benefits, also has drawbacks. Each sensor has aforementioned intrinsic resistance and capacitance and with increasing ladder length, the capacitance/resistance also increases. These length dependent components will intrinsically add noise to the system and will be the limiting component to this detector. A comprehensive study of the noise contributions and limitations of the long-ladder is the subject of this thesis.

3 Noise and Methodology

3.1 Noise

Noise, in the context of electronics, is random fluctuations in the readout signal due a variety of environmental and systematic sources. For readout electronics, keeping the noise at a reasonable level is vital to be able to recognize charge deposition signals. In detector physics a signal to noise ratio (S:N) of at least 12:1 is essential to distinguish the signal from the noise, as well as determine various information from the signal. This ratio derives from the fact that it is infeasible to record the state of every channel of the detector for each beam crossing, and consequently we only want to record channels for which a passing particle left a signal, suppressing the channels that merely have noise in them. We do this by applying a threshold in the electronics high enough above the noise to suppress noise hits but far enough below the mean signal to maintain efficiency.

For detectors, there are two broad sources of noise, environmental noise and inherent noise coming from the system. Environmental noise, such as electromagnetic waves, can lead to consistent degradation of the S:N ratio and disrupt the sensitive electronics of the readout chip. These environmental effects can be mitigated with arrays of shielding with metallic structures and avoiding ground loops. On the other hand, inherent system noise cannot be eliminated, but only controlled once its sources are understood and quantified.

To fully understand the noise contributions of this long-ladder detector, a concrete understanding of inherent noise sources in silicon sensors is an essential prerequisite. Helmuth Spieler showed the square of readout noise, given in SI units, is [4]

$$Q^2 = F_i\tau\Big(2eI_d + \frac{4kT}{R_b} + i_{na}^2\Big) + \frac{F_vC^2}{\tau}\Big(4kTR_s + e_{na}^2\Big) + 4F_{vf}A_fC^2 \tag{1}$$

where Q is the readout noise in Coulombs. This is a simplified equation under the assumption the resistance and capacitance of the detector are separated "lumped" elements, and not spread continuously as they are in a true network.

I_d is the leakage current, discussed below; R_b the value of the bias resistor which grounds the p-implants; T , the temperature in kelvin; R_s, the resistance of one strip in the ladder, and C, the capacitance of one strip of the ladder to its two nearest neighbors and the backplane. F_i, F_v, and τ depend on the shaping parameters of the amplifier. The definition of F_i,F_v are

$$F_i = \frac{1}{2\tau}\int_{-\infty}^{\infty}[W(t)]^2dt \tag{2}$$

$$F_v = \frac{1}{2\tau}\int_{-\infty}^{\infty}[\frac{dW(t)}{dt}]^2 dt \tag{3}$$

where $W(t)$ is the voltage excitation function of the amplification chain. i_{na} and e_{na} are the current noise and the voltage noise of the LSTFE ASIC, respectively. A table of these values for the LSTFE chip and attached sensor can be found in Table 3.1.

To mimic the long-ladder detection scheme, a resistive sensor was chosen such that the noise was primarily dependent on length driven terms of equation 1. Because the capacitance and resistance of the sensor load increases by adding each step of the ladder, it is natural to concentrate on noise sources that depend on the ladder length, although we'll need to understand all significant sources. One length dependent noise, stemming from thermal sources, is referred to as Johnson noise and arises by the thermal motion of electrons in resistors. The length dependent Johnson noise is the voltage-reference noise feeding into the capacitance C, giving a charge noise. Moreover, the total Johnson noise contribution from the resistive sensor can be described as

$$e^2 = 4kTR_s \tag{4}$$

where k is Boltzmann's constant, T is temperature, and R_s is the resistance of the detector. [4]. A second Johnson noise source will be discussed later in this section.

The e_{na} term in equation 1 refers to the random voltage excitations of the amplifier feeding into the sensor capacitance, again leading to a charge noise. Because of our choice of resistive sensors, the $\frac{F_v C^2}{\tau}\left(4kTR_s\right)$ and $\frac{F_v C^2}{\tau}\left(e_{na}^2\right)$ terms are going to be the most dominant at high ladder length as these terms in the equation grow as a function of both $C^2 R_s$ and C^2. These two terms will be studied in detail and simulated as a distributed network rather than separately lumped.

Another length-dependent source of inherent noise is due to the intrinsic properties of diode-like devices, such as these p-implanted, n-type silicon sensors. Called dark current or leakage current, this noise arises from quantum fluctuations at the P/N junction. Each additional strip added to the ladder provides an additional leakage current source of noise to the readout scheme. For well manufactured devices, the leakage current increases with bias voltage eventually saturating at some small value. Nonetheless, the noise which arises due to the leakage current is seen as

$$i^2 = 2eI_d \tag{5}$$

where I_d is the leakage current, and e is the fundamental charge of an electron in Coulombs [4]. Integrated over the shaping time of the electronics, this leads to a current noise charge of $\tau 2eI_d$, seen as the first term of equation 1. Although not a dominant source of noise for high-quality sensors, we will nonetheless consider it as we develop our model of the sensor and readout.

A type of length-independent noise is called 1/f noise, or flicker noise. Particularly dominant at low frequencies, this noise is not random, unlike the previous noise sources and emerges as charge carriers are trapped and released. When a particle traverses the detector, creating 25,000 electron/hole pairs, these charge carriers can be trapped for various times, then released. The staggered release times introduces a noise density which is inversely proportional to the frequency [4]. The trapping rate generally rises with irradiation and is accounted for by the A_f variable in the last term. For unirradiated and low radiation environments, as in the ILC, this contribution is small, and thus this last term is irrelevant.

Table 3.1: Amplifier and Detector Properties

$I_d\ (1strip)$	$0.27\,nA$
R_b	$44\ M\Omega$
$R_s\ (1strip)$	$287\ \Omega$
$C\ (1strip)$	$5.2\,pF$
F_i	1.47
F_v	0.48
τ	$1.06\ \mu s$

The other Johnson noise contribution is from the bias resistor, R_b. This noise,

$$i^2 = \frac{4kT}{R_b} \tag{6}$$

is the current noise from the bias resistor. This noise is integrated over the shaping time, once again giving a charge noise, though this time inversely proportional to the resistor. Because of the large resistance of this R_b, 44 $M\Omega$, this term is negligible.

Overall, the most dominant term at large ladder lengths is the C^2R_s term. Consequently, it was expected the noise squared grows as a function of l^3, or $Q \sim l^{\frac{3}{2}}$ in the long-ladder limit.

3.2 Comparison with the Naïve Model

The noise measured on the physical setup by our group did not match the analytical expectations of equation 1 [5]. This can be seen in Figure 7, where the red line is the values of noise measured as a function of ladder length, and the blue line is the noise expected via equation 1. Clearly, the analytical model is an inaccurate representation, more so at longer ladder lengths. This is due to the assumed distribution of material in the detector and the reduction of noise may in fact be attributed to networks effects. In a real detector, the strip resistance and capacitance are distributed throughout the detector, but equation 1 assumes a single "lump" of resistance and capacitance. These network effects and assumptions of equation 1 are explored in this thesis.

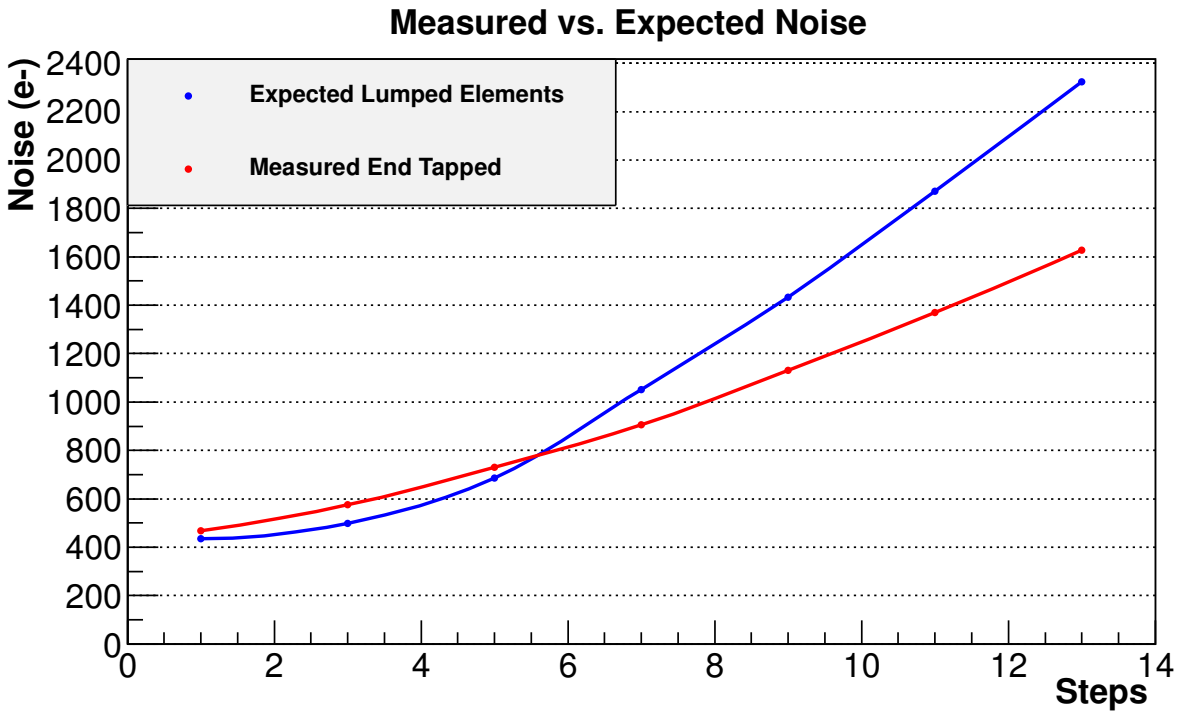

Figure 7: A plot of measured and expected noise values as a function of ladder length

Implementing this distributed model in a calculation can be quite a daunting task; instead, inspired by this intriguing behavior of the noise, prior undergraduate Aaron Taylor began the development of a SPICE (Simulation Program with Integrated Circuit Emphasis) model in order to better understand finer details of the noise elucidate discrepancies between the expected noise and measured noise.

Taking the bare-bones model fashioned by the group, I completed the development of the SPICE model, tuning the model to various empirical inputs constraining the LS-

FTE chip performance and sensor properties, and studied different physical phenomena of the setup. Taking prior measurements, I performed semi-empirical simulations to probe understandings about the discrepancies between the naïve expectation and the physical setup. A full description of the SPICE model is presented in the next section.

3.3 The SPICE Model

The SPICE model is split up into three basic parts of the charge injection scheme, detector, and readout — seen in the next couple pages. Note: the schematics presented include additional corrections to be discussed in the next section.

In the physical testing, to mimic the typical amount of charge traversing particles would deposit, 2 femtocoulombs would be injected into the detector by using a pulsar to send a voltage step across an input capacitor [5]. A simplified SPICE injection scheme is used to transfer 2fC to the system (Fig. 8).

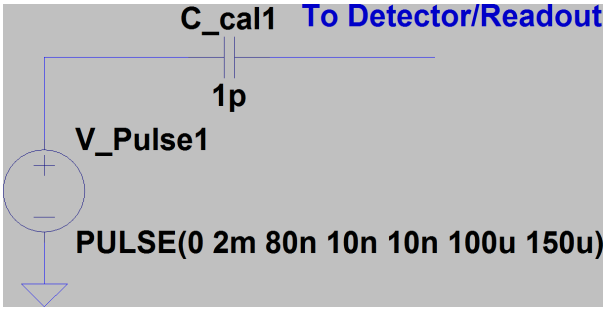

Figure 8: The circuit diagram of the pulse injection system present in the SPICE program. The pulses were setup to match the physical setup

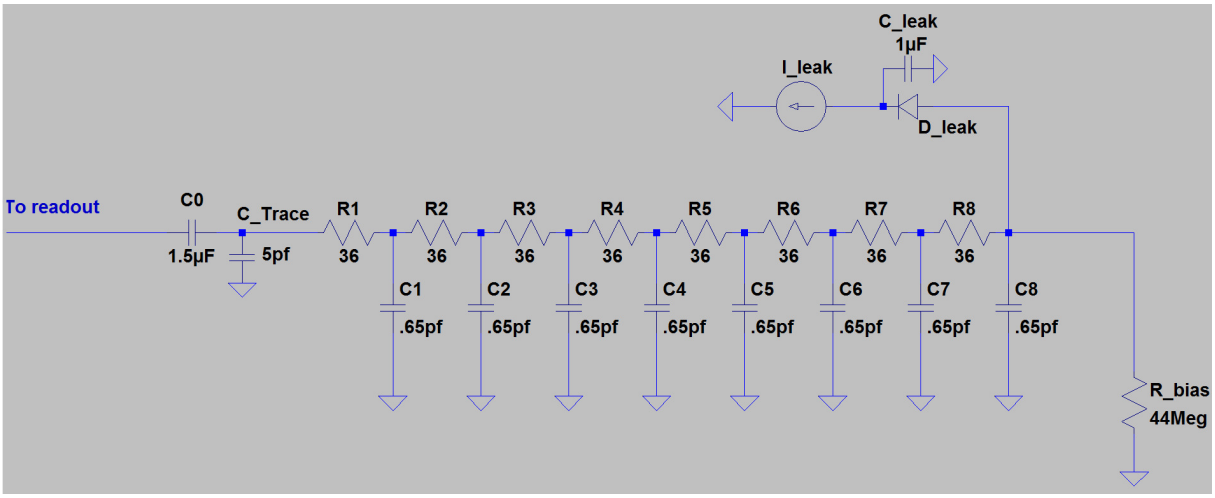

Figure 9: The sensor load network for one step of the long-ladder divided into 8 segments such that the total resistance and capacitance is the same as the naïve lumped model

Since the lumped element approximation of equation 1 is a poor fit for long-ladders,

it was natural to not model the detector as a single resistor and single capacitor to ground. It was shown that dividing the continuous physical detector into a network of eight discrete RC circuits was a sufficient approximation of a continuous, distributed RC network. Further division of the sensor yielded negligible improvements — a change in noise of $<$0.1% when increasing the number of RC circuits from 8 to 16 [6]. Since the resistance and capacitance of each step had to be the same as that measured for the sensor, the resistance and capacitance of each RC circuit was set as one eighth of the whole sensor.

A single ladder of the detector is shown in Figure 9. In the end-tapped configuration, additional steps of the ladder would just be placed in series, so for the final test of 13 steps, there would be a total of 104 discrete RC circuits elements. Figure 10 shows the circuit in the two-step,center-tapped configuration in which half of the strips are on each side of the path to the readout electronics.

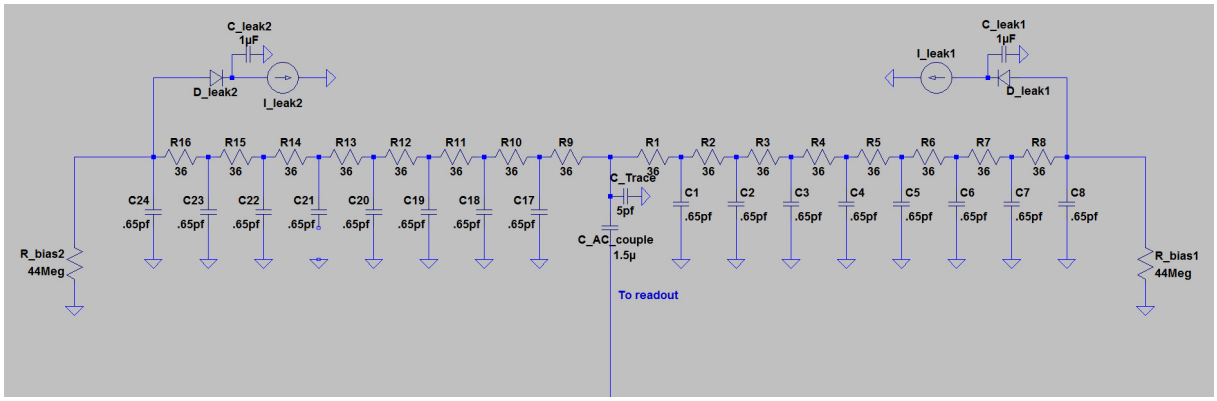

Figure 10: Two steps of the long-ladder read out in the center-tapped configuration. For the last measurement of 13 steps, one side had 6 steps, and the other side had 7

The final part of the SPICE model is the LSTFE ASIC readout electronics. Figure 11 shows the schematic for the LSTFE readout chain. It consists of the preamp and shapers (differentiation and integration stages) discussed previously.

SPICE simulates under ideal conditions, so additional noise was added to the operational amplifier due to the intrinsic noise of the amplification chain. This value in equation 1 is the $\frac{e_{na}^2}{\tau}$ part of the second term. In the equation the e_{na}^2 term is multiplied by the capacitance, and consequently can be independently constrained by measuring the noise vs. capacitance for purely capacitive loads. In SPICE this is accounted for by a 1 $m\Omega$ resistor labeled R_{noise}. This dependence was measured in the physical setup and seen to be 9.1 electrons per picofarad (Fig. 12). This noise was added to the ampli-

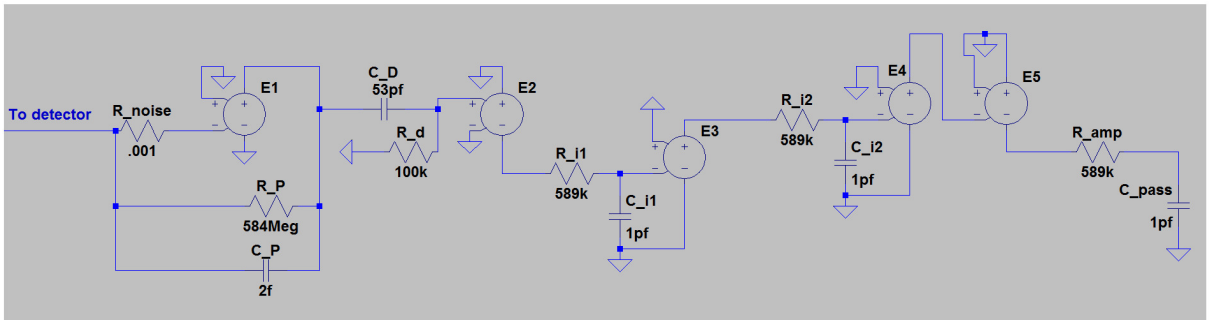

Figure 11: The LSTFE readout chain in the SPICE simulation. R_{noise} is the added noise resistor to add the intrinsic noise of the amplification process

fication scheme with R_{noise} by tuning the temperature of it, and the placement of this resistor was chosen so that it did not affect any property of the amplification, except for the noise.

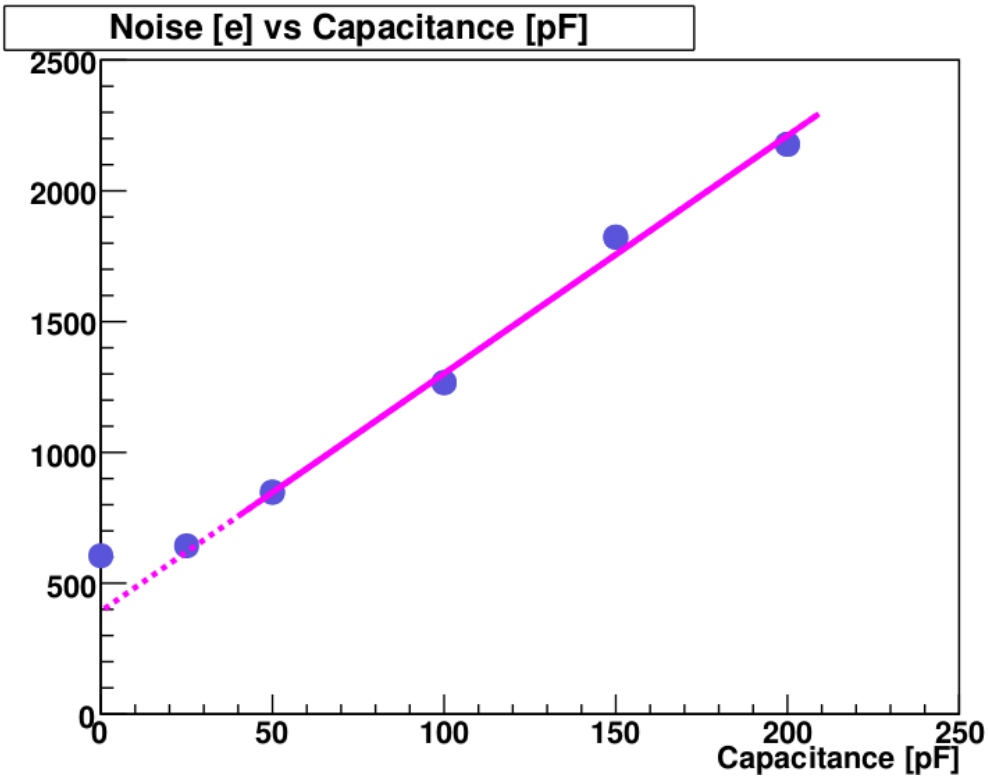

Figure 12: Noise slope of the LSFTE amplifier measured. A slope 9.1 $\frac{e}{pF}$ was measured for purely capacitative loads [5]

4 Refinement of the SPICE Model

4.1 The Amplification Chain

Much of the work detailed in this thesis includes refinement of the SPICE model to incorporate independent empirical inputs and additional corrections associated with the practical aspects of the instrumentation and readout of the sensor. This section describes the various stages of the refinement.

To achieve a readout simulation, it was necessary to match the gain, stability, rise time, and shaping time of the SPICE amplifier to that measured with the setup. The rise time, defined as the time it takes for the pulse to go from 10% of its maximum height to 90% of its height, and shaping time were measured to be $1.060\mu s$ and $1.8\mu s$ respectively [5]. I adjusted the resistance and capacitance values of the integrators to match this time to the simulated values, while keeping the gain and stability of the gain as close as possible to previous versions of the SPICE setup. The temperature of the noise resistor was then readjusted to to match the 9.1 $\frac{e}{pF}$ measurement seen in Figure 12. I found a temperature of 250 Kelvin for R_{noise}, in tandem with the new adjusted amplification scheme, gave the best agreement between the SPICE simulation and the physical setup.

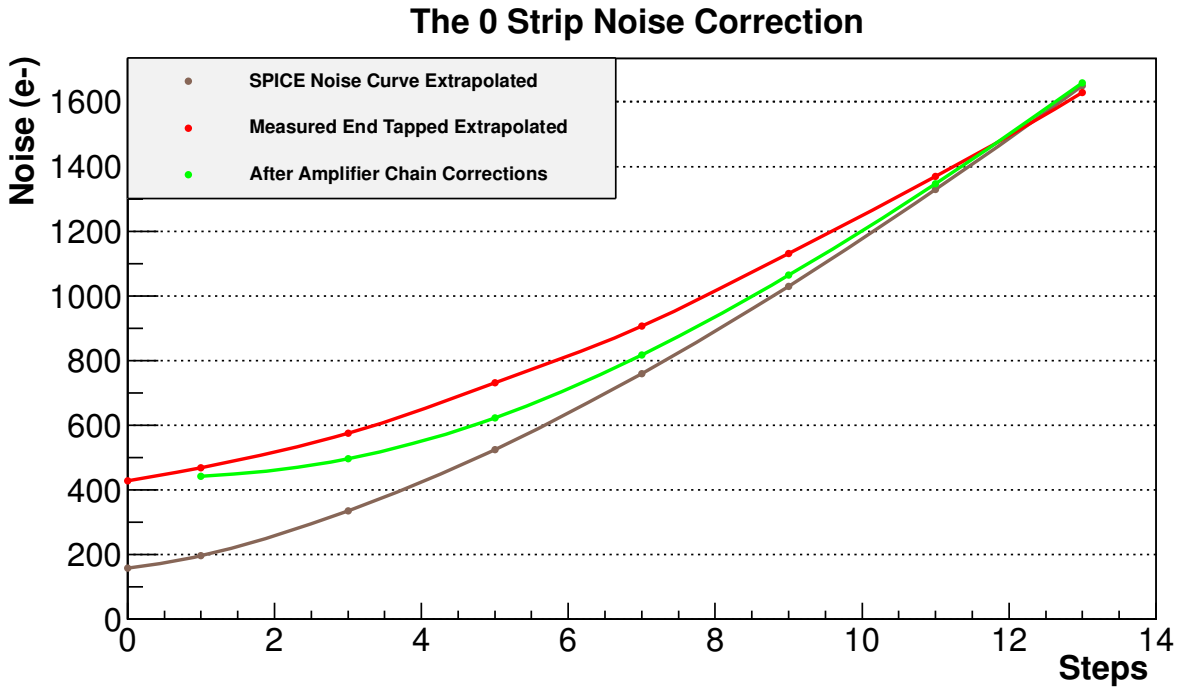

Figure 13: The 0 strip SPICE model noise before and after amplifier chain corrections and measured noise. Agreement good except for short to moderate lengths

After tuning the shaping of the readout, the simulations matched the measured values of noise well at high ladder length, but poorly at low to middle ladder length. One key element the model lacked was the noise due to the LSFTE current noise contribution, i_{na} in equation 1. At this point in the development, the SPICE model would yield 0 noise in the limit of 0 ladder length, while in fact there is a non-zero noise, primarily from the LSTFE current noise. To incorporate this into the model, a power law least square fit was made to the SPICE and measured noise curves and extrapolated down to zero strips. The value of noise between the model and the measurement was then added in quadrature to every point, adjusting the original brown line to the new green line in Figure 13.

4.2 Sensor and Readout Capacitance

As seen in the figure, the fit now seems to be much better except for the discrepancy at short to moderate ladder lengths. This variation could arise from a lack of understanding of the network or strip effects, or even some things forgone in the simulation. In order to assess what possible sources could be contributing to this "belly", I tried changing the model in order to incorporate miscellaneous properties associated with the physical setup.

The physical sensor was read out with the LSTFE, which was mounted on a specifically designed PC board. Traces, electrically conducting pathways allowing signals to propagate on the PC board, have a small capacitance to ground. While this trace capacitance was small ($\sim$ 5 pF), it was thought this small capacitance at low ladder lengths might introduce a non-negligible noise source. This trace capacitance was added as an extra capacitor to ground between the readout and the detector. It can be seen in both circuit schematics — Figures 9 and 10. This seemed to reduce the "belly" a small amount.

Another idea we had related to values of the sensor capacitance. The capacitance of the sensor was quoted to be 5.2 $\frac{pF}{strip}$, but processing uncertainties made this value only exact up to $\pm 5\%$. Changing the capacitance values of the strip by 10% in each direction would show the dependence on the capacitance, and if it affected this "belly" in any way, I could then go into further detail of tuning this uncertainty. This study was also a good way to verify our $l^{3/2}$ assumption, as changing the capacitances by a significant amount would affect the most dominant term in the equation, $\frac{F_v C^2}{\tau}\left(4kTR_s\right)$. We expected to see the most drastic changes at higher ladder length.

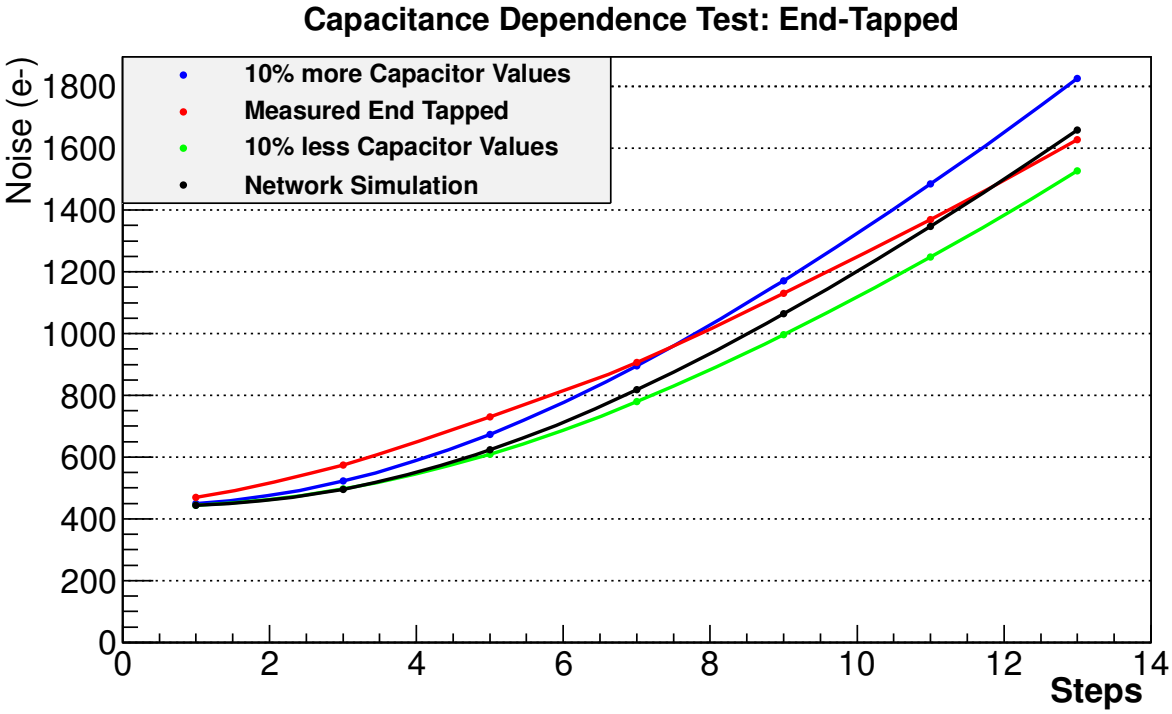

Figure 14: A plot showing the difference in noise values when changing the values of the capacitors by 10%

Seen in Figure 14, one can clearly see the capacitive effects are much greater at larger ladder lengths, but changing the values in either direction did very little to mitigate the discrepancy of the "belly". While this strengthened our faith in the our effort to constrain the limiting behavior we sought to study, it cast no light on the origin of this disparity at low and middle ladder lengths.

4.3 The Bias Resistor

The bias resistor was another static circuit component studied which contributes to the noise of the detector. A high-valued resistor of 44 $M\Omega$, the bias resistor's job is to keep the p-implants connected to a ground potential. The larger the value the less current is running through the resistor,thus current noise generated by the bias resistor is reduced. According to the equation 1, the $F_i\tau\left(\frac{4kT}{R_b}\right)$ term — the one including the value of the bias resistor — will be more dominant at lower strip lengths before the capacitance/strip resistance term starts to takeover.

To bracket the importance of this bias resistance term, I changed the value of it in

the SPICE simulation by factor of 10 in each direction, examining the noise dependence on this term. There was a change of less than five electrons for both cases. Given that a factor of 10 difference did very little to alter the noise contributions, there was no use further investigating this term. Looking back at the $F_i\tau\left(\frac{4kT}{R_b}\right)$ term, it could be seen this would have been expected to make little change because that term has a factor of Boltzmann's constant, which is of order 10^{-23}, divided by an large value, R_b, while the other terms which have this constant multiplied by a large number growing with the length of the ladder.

4.4 Leakage Current

Discussed earlier, the leakage current arises due to quantum fluctuation at the sensor P/N junction creating a current inside the depletion region, opposite the direction of normal current flow. The leakage current of the physical setup was measured to be 0.27 nA per strip. According to equation 1, at short to middle range ladder lengths, the noise should not be completely dominated by the $l^{\frac{3}{2}}$ term. This allows for the possibility of an added noise source to come into play and contribute significant noise. Leakage current seemed like a promising candidate to explore.

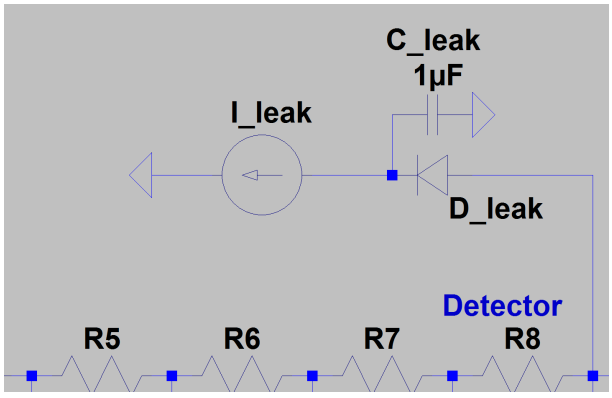

Figure 15: A diagram of the scheme created to administer leakage current without disturbing the system

Adding this value of current to the SPICE model required the development of an additional simulation technique. Initially, it seemed like an easy task by just adding additional current sources to the beginning each set of 8 RC networks. SPICE handled this a different way than expected, changing the other aspects of the model such as the shaping time of the readout. Going back to the drawing board and with the help of engineer Edwin Spencer of the Santa Cruz Institute of Particle Physics (SCIPP), we created the device seen in Figure 15. Using a reversed diode, with a specific tunable current, we could administer the measured amount of leakage current, while limiting the impact on other aspects of the simulation.

Seen in Figure 16, the leakage current has a significant effect on the noise values

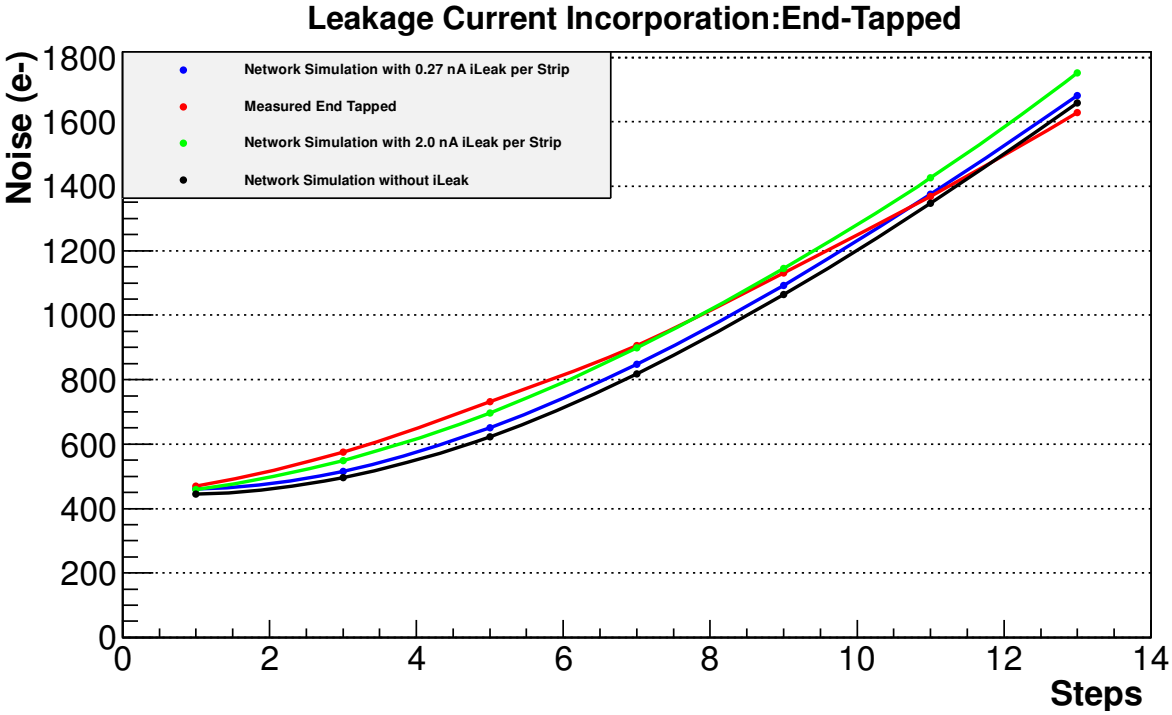

Figure 16: The 0 strip noise correction to the SPICE model. The measured and SPICE noise curves are extrapolated down to 0 strips, then the difference is added in quadrature to each point

at low to medium ladder length. The entire belly can be essentially reconciled with the measured data with a purely unphysical value of 2.5 nA. The value of 0.27 nA measured, does help resolve this discrepancy, but minimally. It does in fact increase some of the noise values by as much as $\sim$2% in the low to middle range ladder lengths, and only contributes to less than half a percent to the larger ladder lengths. So while we see the qualitative behavior we would expect, the quantitative results provide little change, but change nonetheless, in the right direction.

5 Results

5.1 End-Tapped

After completing the model, refining the model, and incorporating known noise sources the final results are presented below (Fig. 17). The naïve expectation of the lumped model is presented as the blue line. The red line is the measured noise levels and the green line is the full network simulation of the SPICE model. The distributed 8 RC circuit model agrees much better with the measured results prediction than the Spieler lumped element description. Overall, the SPICE model provided a good, a-priori representation of the noise dependence on ladder length.

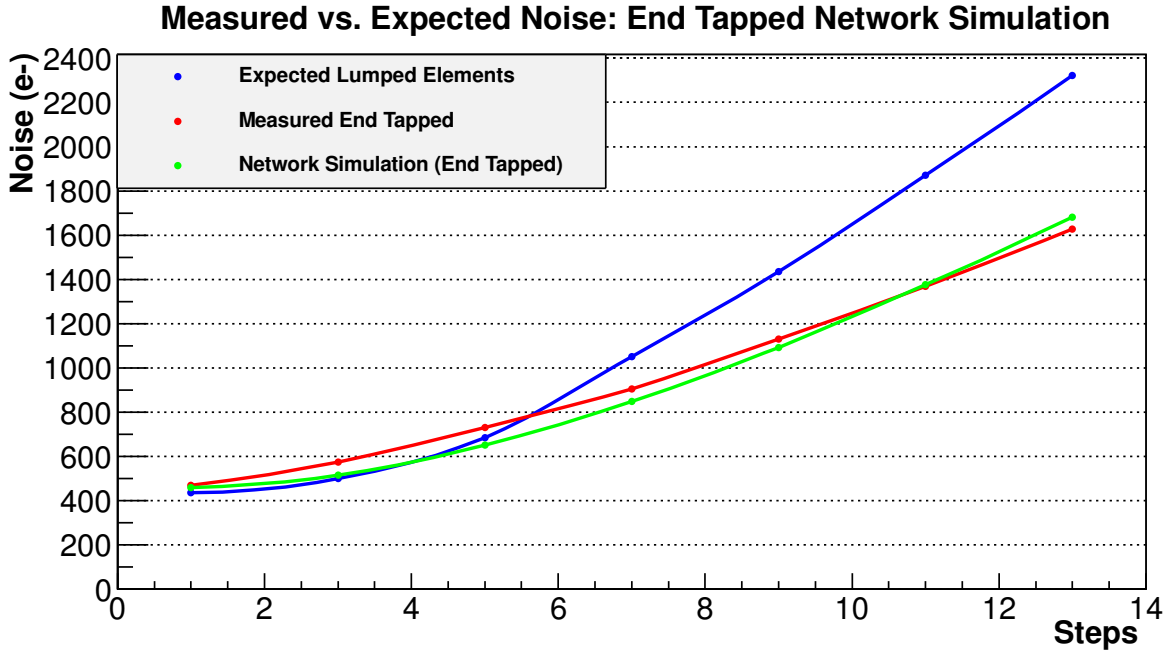

Figure 17: A plot showing the end-tapped results. This final model includes physical properties such as the trace capacitance and the leakage current

Seeing as the noise is much lower than the lumped model, this confirmed our suspicions that networks effects play a large role in mitigating the readout noise from the sensor. This is good news as it could allow for longer than envisioned ladder length and gives us confidence in our model for high ladder lengths, where we expect the noise to be load dominated.

There is just one small disagreement at low ladder lengths. It was noted in the leakage current studies that this discrepancy can be resolved if one assumed a leakage current ten times that of what was measured for the sensors. Thus, there could possibly

be undetected sources of leakage current. However, it should be noted that this has no effect on the noise at the largest ladder lengths are the resistive and capacitances of the detector are the main noise source contributions.

5.2 Center-Tapped

The preceding studies and guidance provided by equation 1 indicate the noise coming from the detector load is the primary contributing element to the total readout noise. In order to reduce this effect, one could potentially read out of the detector from halfway through the daisy-chain. That is to say, instead of having the readout electronics on the end of the detector, we could put the readout electronics with half of the strips on one side, and half on the other side. This would be equivalent to reading out the load in two parallel paths. Half the resistance would be in parallel, making the total resistive load seen by the LSTFE $\frac{R}{4}$ instead of R. This reduction would only occur in the $\frac{F_v C^2}{\tau}\left(4kTR_s\right)$ term of equation 1, although network effects might modify this.

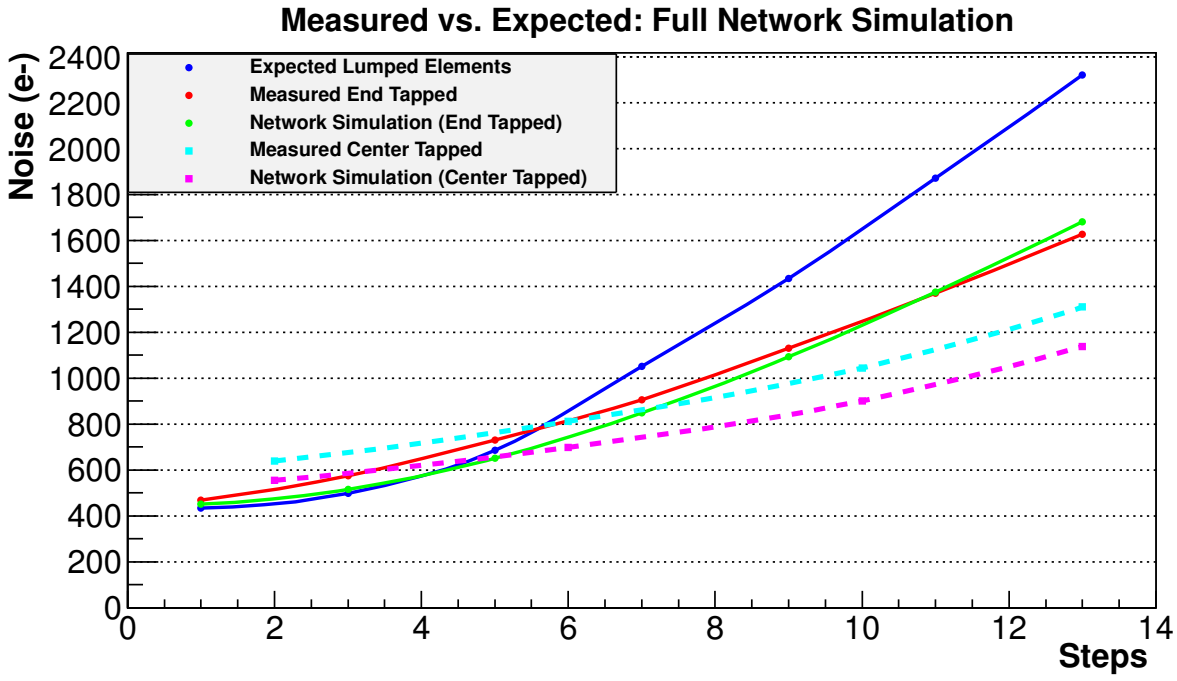

Figure 18: A plot showing the cente-tapped results. Note the reduction of noise at long ladder lengths

Physical measurements were performed for ladder lengths of 2, 6, 10 and 13 steps and are compared with simulated results above. For the 13 step ladder, the detector was portioned into two ladders of unequal lengths of 6 and 7 steps. Seen in Figure 18,

there is a significant reduction in noise compared with the conventional end-readout senors. The results shown are for center tapped sensors, with the additional corrections of trace capacitance and leakage current added into the model. Despite this relative noise mitigation there is one caveat — the model for center tapped readout is slightly less understood as seen by the consistent disagreement between the simulation and measurement. Variation of the model parameters within expected uncertainties didn't achieve significantly better agreement. Even so, it is observed qualitatively that center-tapping the readout reduces the noise present in the long-ladder system and clearly shows better performance.

6 Summary and Outlook

Using single channel electronics that incorporates the LSFTE ASIC to read out 10's of sensors "daisy-chained" together, the long-ladder scheme can potentially reduce electrically noise, scattering due cabling, and costs of the microstrip tracking region of the SiD. Assessing the noise limitations of this detectors is vital in determining if it can be considered as a viable candidate, given the remarkable precision and efficiency requirements of the ILC collaboration.

With the help of a SPICE simulation of the long-ladder system, aspects of the physical model and the difference with the naïve lumped element model were investigated. Important, previously unaccounted for elements such as leakage current and trace capacitance were added to the model. Further tuning of the LSTFE amplification chain improved the model's reflection of physical setup.

The readout noise for the end-tapped configuration as a function of ladder length, presented in this paper, are significantly below the expectations of the naïve lumped element model. This is primarily due to the important role of network effects in mitigating the readout noise. Furthermore, reading the system out in the center-tapped configuration reduces the noise even more at large ladder lengths. This is good news for the long-ladder as at very long ladder lengths, networks effects and reading the sensor out in the center-tapped configuration will play a role in keeping the noise at tolerable levels. While the SPICE simulation shows good agreement between simulation and measurement for the end-tapped configuration, further thought should be aimed at the center-tapped configuration in order to clear up the discrepancy.

With this design implemented, the long-ladder could potentially reach lengths of up to 1 meter, reducing the amount of readout electronics by at least a factor of 10. Across the board, the long-ladder detection scheme looks like a promising candidate for the microstrip tracking region of the SiD.

Acknowledgements

First and foremost, I would like to thank Bruce Schumm, my advisor. I came to him knowing nothing about particle physics and electronics, but over the last 3 years, I have learned a plethora of interesting and exciting experimental methods and problem-solving approaches.

Next I would like to thank Vitaliy Fadeyev, Max Wilder, and Ned Spencer. Without all their support, I would not know nearly as much about front end electronics, signal processing, and detectors. Without them, my progress with all the projects I worked on, especially this one, would not at all have been possible.

I also want to thank the past and present ILC R&D group members — London Chappellet-Volpini, James Maduzia, Neil McFadden, Omar Moreno, Spencer Ramirez, Sheena Schier, Aaron Taylor, and anyone I may have forgotten. They were people who made the lab work interesting and exciting, and we all had problems of coding, equipment, or classes we could complain about together. Particularly, I want to thank Aaron Taylor and Sean Crosby, who got this project off the ground, laying a foundation for me to work with.

References

[1] Singer, Charles.*A Short History of Science to the 19th Century*, Streeter Press, 2008.

[2] CERN Press Office. *CERN experiments observe particle consistent with long-sought Higgs boson*, 2012. [Press release].

[3] *International Linear Collider Design Reference Report. Vol 4: Detectors*, August 2007

[4] Spieler, Helmuth. *Semiconductor Detector Systems*, Oxford University Press, New York, 2005.

[5] Crosby, Sean. *Investigation of Silicon Sensor Strip Noise on Long Ladders*, Undergraduate thesis, Santa Cruz, 2009.

[6] Taylor, Aaron. *A Spice Study of Silicon Sensor Strip Noise on Long Ladders*, Undergraduate thesis, Santa Cruz, 2011.